Twelve Loci Associated With Bone Density in Middle-aged and Elderly Chinese: The Shanghai Changfeng Study

Hailuan Zeng,[1,2,3,*] Jieyu Ge,[4,*] Wenjie Xu,[5] Hui Ma,[6] Lingyan Chen,[6] Mingfeng Xia,[1,2] Baishen Pan,[7] Huandong Lin,[1,2] Sijia Wang,[4,8] and Xin Gao[1,2,3]

[1]Department of Endocrinology and Metabolism, Zhongshan Hospital, Fudan University, Shanghai, China
[2]Fudan Institute for Metabolic Diseases, Shanghai, China
[3]Human Phenome Institute, Fudan University, Shanghai, China
[4]CAS Key Laboratory of Computational Biology, CAS-MPG Partner Institute for Computational Biology, Shanghai Institute of Nutrition and Health, Shanghai Institutes for Biological Sciences, University of Chinese Academy of Sciences, Chinese Academy of Sciences, Shanghai, China
[5]State Key Laboratory of Genetic Engineering and Ministry of Education Key Laboratory of Contemporary Anthropology, Collaborative Innovation Center for Genetics and Development, School of Life Sciences, Fudan University, Shanghai, China
[6]Department of Geriatrics, Zhongshan Hospital, Fudan University, Shanghai, China
[7]Department of Laboratory Medicine, Zhongshan Hospital, Fudan University, Shanghai, China
[8]Center for Excellence in Animal Evolution and Genetics, Chinese Academy of Sciences, Kunming 650223, China

Correspondence: Xin Gao, MD, Department of Endocrinology and Metabolism, Zhongshan Hospital, Fudan University, no. 180 Fenglin Road, Shanghai 200032, China. Email: zhongshan_endo@126.com; or happy20061208@126.com; or Sijia Wang, PhD, CAS Key Laboratory of Computational Biology, Shanghai Institute of Nutrition and Health, University of Chinese Academy of Sciences, Chinese Academy of Sciences, no. 320 Yueyang Road, Shanghai 200031, China. Email: wangsijia@picb.ac.cn; or Huandong Lin, PhD, Department of Endocrinology and Metabolism, Zhongshan Hospital, Fudan University, no. 180 Fenglin Road, Shanghai 200032, China. Email: lin.huandong@zs-hospital.sh.cn.
*These authors contributed equally.

Abstract

Context: Previous genome-wide association studies (GWASs) of bone mineral density (BMD) were mainly conducted in Europeans.

Objective: To explore genetic variants that affect BMD and sex differences in a Chinese population.

Methods: A total of 5428 middle-aged and elderly Chinese were included. Dual-energy X-ray absorptiometry was used to measure BMD at the lumbar spine, and total and specific sites of the hip. A mixed linear model was used to analyze the associations between BMD and autosomal genetic variants, adjusting for age, age squared, sex, and menopausal women (model 1); model 2 was further adjusted for height and weight. A GWAS of osteoporosis in the Biobank Japan (BBJ) project was used for replication. GWAMA software was used to detect the statistical significance of sex differences of estimated effects. Gene annotation and pathway enrichment analysis were performed.

Results: Women lost BMD at earlier ages and faster than men. The 2 models identified a total of 12 loci that were associated with BMD at any site. Single nucleotide polymorphisms rs72354346, rs2024219, rs1463093, rs10037512, and rs5880932 were successfully replicated in the BBJ. Variations of rs79262027 G>A (*VKORC1L1*) and rs4795209 A>G (*DDX52*) were associated with BMD only in men, and rs1239055408 G>GA (*KCNJ2*) was associated with BMD only in women. Gene enrichment analysis showed that BMD in a Chinese elderly population was mainly related to ossification, bone resorption, sex hormones, and kidney physiology.

Conclusion: The present GWAS identified 12 loci that were significantly associated with BMD at any site in a Chinese population, and 3 of them showed sex differences in their effects.

Key Words: bone mineral density, genome-wide association study, sex interaction, East Asian

Abbreviations: BBJ, Biobank Japan; BMD, bone mineral density; DXA, dual-energy X-ray absorptiometry; eQTL, expression quantitative trait locus; GRM, genetic relationship matrix; GO, gene ontology; GWAS, genome-wide association study; MAF, minor allele frequency; M(eff), effective number; PC, principal component; SNP, single nucleotide polymorphism.

Osteoporosis is an aging-related condition characterized by low bone mineral density (BMD) and microarchitectural deterioration of bone tissue, resulting in bone fragility and increasing risk of fractures (1). It is a highly prevalent metabolic bone disease estimated to affect 13% of the Chinese population (2), and the age-standardized prevalence is about 6.46% and 29.13% for men and women aged 50 years and older in China (3). Previously, we found that

osteoporosis is an independent predictor of all-cause mortality in a middle-aged and elderly Chinese population with a population attributable risk percentage of 11.7% (4).

BMD has an estimated heritability of 50% to 80% (5). Genome-wide association studies (GWASs) and meta-analyses have discovered hundreds of susceptibility loci for BMD, osteoporosis, or fractures (5). Early studies with relatively small sample sizes have found or validated some

susceptible genes with greater effects, such as *ESR1*, *LRP5*, *PPARG*, *CYP19*, *SP7*, *SOST*, *MARK3*, *RANKL*, *TNFRSF11A*, *ZBTB40*, and so on. The GEnetic Factors for OSteoporosis (GEFOS) consortium carried out GWAS meta-analysis of several European cohorts with sample sizes from 19 195 to 66 628 and identified more than 60 new loci that were associated with BMD, explaining about 6% of BMD variation (6–9). Another remarkable work is the UK Biobank project, in which 153 and 301 new loci were identified to be associated with ultrasound-measured heel-estimated BMD in more than 140 000 and 420 000 participants respectively, explaining nearly 20% of BMD variation (10, 11). These studies, however, were mainly performed in European populations, and there exists heterogeneity between BMD measured by different types of methods and at different skeletal sites. Only a few GWASs have focused on East Asian populations, but their sample sizes were relatively small (<3000) (12–17).

Sex differences in bone characteristics including bone density, bone strength, bone geometry, and osteoporotic fracture rates are well established (18). Women lost bone mass rapidly after menopause with trabecular number decreased and cortical porosity increased, whereas men lost trabecular thickness with aging (18, 19). Elucidating sex-specific gene effects on BMD may shed light on the pathogenesis and therapeutic targets of osteoporosis.

In the present study, we aim to identify genetic variants associated with BMD at multiple skeletal sites measured with the gold standard, dual-energy X-ray absorptiometry (DXA), in the middle-aged and elderly Chinese population of the Shanghai Changfeng Study. We also tested single nucleotide polymorphism (SNP) by sex interaction effects of the identified SNPs.

Materials and Methods

Study Population
During 2009 to 2012, a total of 6595 middle-aged and elderly (≥45 years old) Chinese participants from Shanghai Changfeng Community were recruited by the Shanghai Changfeng Study (4, 20). Participants answered standard questionnaires relating to menopausal status (for women), health history, lifestyle, and medication, underwent physical measurements, and provided biological samples. Among them, 6203 participants underwent DXA scans. We excluded 304 participants who had received treatments that might influence bone metabolism (eg, hormone replacement therapy, anti-osteoporotic drugs) in the 1 month before blood draw or who had self-reported thyroid diseases or parathyroid diseases, and 24 participants whose information on age, sex, or menopause was missing, resulting in 5875 participants passing the phenotype quality control (QC). Among the 6595 participants enrolled, 5689 had DNA samples and were genotyped at baseline. During 2014 to 2017, we conducted a follow-up survey, and another 433 DNA samples that did not overlap with baseline DNA samples were collected. After genotyping QC (see "Genotyping, Imputation, and Quality Control"), 60 of the 5689 participants genotyped at baseline and 9 of the 433 participants genotyped at the follow-up survey were excluded, resulting in a total of 6053 genotyped participants who passed the QC. In genome-wide association analysis of BMD, 5428 eligible participants who had passed both phenotype QC and genotype QC were included in Model 1. In Model 2, another 33 participants missing height or weight were excluded, and the remaining 5395 participants were analyzed (Fig. 1).

Ethics approval was granted by the ethics committee of Zhongshan Hospital affiliated to Fudan University and written informed consent was provided by all participants before participation.

Phenotypic Measurements
Participants underwent whole-body DXA scans and separate scans on the spine and hip, which were conducted by a trained technician using DXA (GE Healthcare Lunar iDXA system) incorporated with enCORE software (version 13.0). BMD (g/cm^2) at the lumbar spine L1 to L4 was derived from spine DXA scans and BMD of the bilateral total hip, femoral neck, trochanter and intertrochanter from hip DXA scans.

Genotyping, Imputation, and Quality Control
Genomic DNA of the participants was extracted from peripheral blood leukocytes using the QIAGEN (Hilden, Germany) QIAamp DNA Mini Blood Kit and genotyped with the Illumina (San Diego, CA, USA) Infinium BeadChip genotyping array (707 180 markers). QC was carried out using PLINK v1.90b4 (21). Samples that had a sex discrepancy between genotypic and reported sex, had a genotype hard call rate <95%, deviated from the expected inbreeding coefficient ($-0.2 < F < 0.2$), or were duplicated were excluded, and markers that had genotype missingness >2%, or Hardy–Weinberg equilibrium $P < 1 \times 10^{-5}$, or minor allele frequency (MAF) <1% were filtered out, resulting in 6053 participants with 426 070 markers.

We performed prephasing and phasing using SHAPEIT v2r790 (22) and imputation with IMPUTE2 v2.3.1 (23) with the 1000 Genomes (1000G) phase 3 data as reference. QC was carried out again, and 8 604 360 variants with call rate >98%, Hardy–Weinberg equilibrium $P > 1 \times 10^{-5}$, MAF >1%, and INFO score >0.8 were included in the final analysis. All genomic positions were in reference to hg19/build 37.

SNP Heritability
SNP-based heritability of BMD at each site in each stratum was estimated using GCTA-GREML analysis in family data implemented in GCTA (24). This method estimates pedigree-based and SNP-based heritability simultaneously in 1 Model using family data without having to remove related individuals.

Genome-Wide Association Analysis
Sex-stratified and combined GWASs were performed for each trait (ie, BMD at each site). BMD values approximated normal distribution, and outliers ≥4 SD from mean were removed separately in men and women prior to analysis. In order to maximize the sample size, we used the mixed linear model in the fastGWA software (25) instead of removing samples due to relatedness. This approach controls population stratification by principal components (PCs) and for relatedness using a sparse genetic relationship matrix (GRM). PCs were calculated with linkage disequilibrium (LD) pruned genotype calls in unrelated participants and projected onto the complete set of 6053 participants (26). Autosomal genetic variants were used to calculate sparse GRM and to test for association with BMD at each site in each
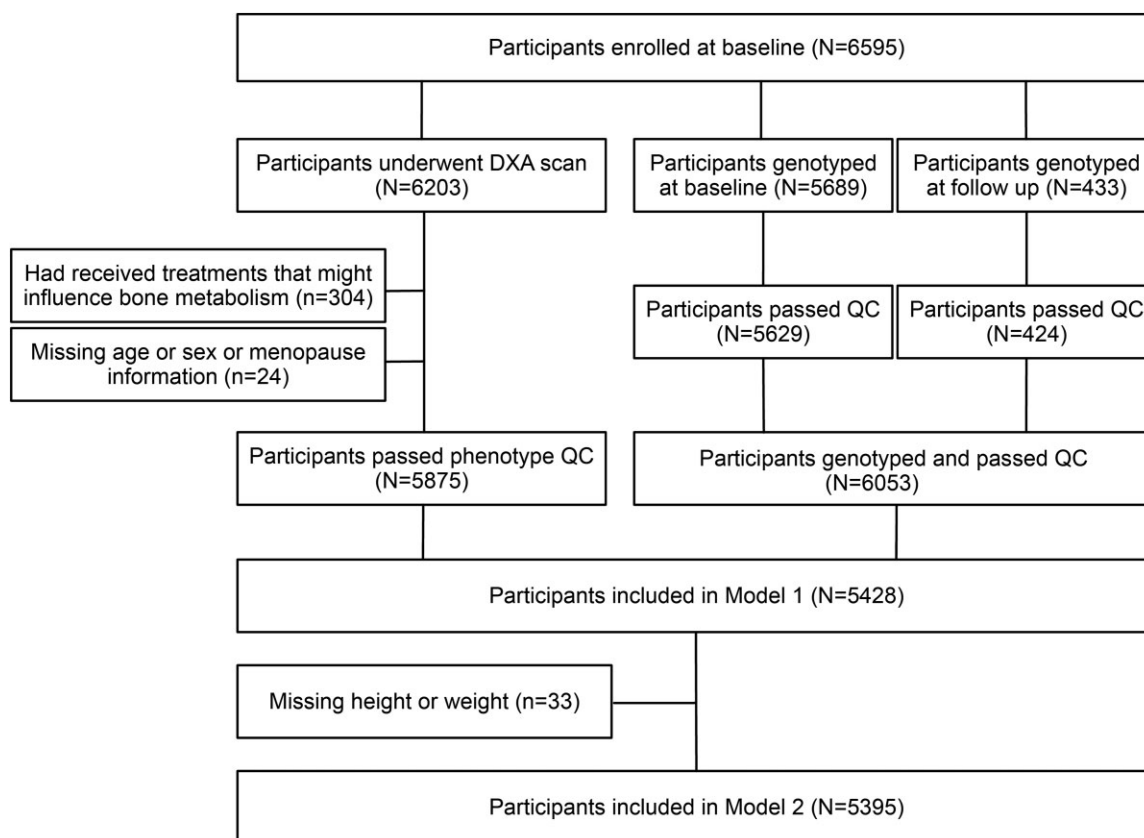
Figure 1. Flowchart of the study participants.

stratum (ie, men, women, and total). Raw BMD values were used as response variables, and autosomal genetic variants were included as random effects. BMD was significantly associated with age, height, and weight in both sexes and associated with menopause in women (see Fig. S1 in (27)). Given the potential for collider bias from using heritable traits as covariates, we conducted GWASs for BMD with and without height and weight as fixed covariates with the assumption of an additive allelic effect: Model 1, adjusted for age, age squared, sex, menopausal women, PCs 1 to 8, and sparse GRM; Model 2, Model 1 plus height and weight. We modeled the covariate effect of sex and menopausal women simultaneously by adjusting the dummy variables transformed from dividing participants into men, premenopausal women, and postmenopausal women. When analyzing women only, we adjusted the covariate effect using menopause as a binary variable.

BMD values at all sites were correlated with each other with Pearson r values ranging between 0.49 and 0.97 (Fig. S1 in (27)). Correlated multiple testing were corrected by calculating the "effective number" (M(eff)) of independent tests (28) followed with Bonferroni correction. M(eff) was calculated by summing the integral and nonintegral parts of each decomposed eigenvalue of the correlation matrix of BMD at the 9 sites, which yielded 3. Therefore, we set $P < 5.6 \times 10^{-9}$ ($5 \times^{-8}$/3 tests/3 strata) as the study-wide significant threshold, and $P < 5 \times 10^{-8}$ as the genome-wide significant threshold.

Interaction Between SNPs and Sex

GWAMA (genome-wide association meta-analysis) software v2.2.2 (29, 30) was used to test for the heterogeneous effects

of the associated lead SNPs between sexes. This method performs sex-combined and sex-differentiated meta-analysis from GWAS summary statistics of men and women. An asymptotically chi-square distributed test statistic was obtained by subtracting the sex-combined squared t-statistic from the sum of the 2 sex-specific squared t-statistics, which is equivalent to a normal z-test of the difference in allelic effects between sexes (30). The gender heterogeneity P value was calculated for each significant SNP in the corresponding models, and $P < .017$ (0.05/3 M(eff)) was considered statistically significant.

Conditional Analysis

Conditional and joint (COJO) association analysis (gcta –cojo-slct –cojo-wind 10 000) (31) was performed for all GWAS summary data to identify independent signals for BMD at each site in each stratum. One locus might be significantly associated with BMD at different sites or in a different stratum but had different lead SNPs, hence we also performed "cross-trait" COJO association analysis conditioning on the most significant lead SNP for those GWAS results that had lead SNPs on the same chromosome with distance less than 10 000 kb.

Regional Association Plots

Regional association plots showing the LD between markers in the prioritized loci were generated using LocusZoom (version 0.14.0) (https://my.locuszoom.org/) (32) with 1000 Genome East Asian (EAS) reference data.

Overlap With Findings From Previous GWASs

Lead SNPs from all independent signals were cross-referenced with the following databases to determine whether they overlapped with previously identified associations from previous GWASs: FinnGen (https://r5.finngen.fi/), GenATLAS (http://geneatlas.roslin.ed.ac.uk/), IEU GWAS database (https://gwas.mrcieu.ac.uk/), and NHGRI-EBI GWAS catalog (https://www.ebi.ac.uk/gwas/). We also carried out PheWAS using PhenoScanner V2 (33, 34) with catalog set to "disease & traits," proxies to "EAS," and LD r2 to 0.6 to search for published phenome-wide associations between our lead SNPs or proxy SNPs and other diseases and traits.

As we were unaware of publicly available GWAS data on BMD, we looked up the lead SNPs in the GWAS summary data of osteoporosis from the Biobank Japan project (BBJ, http://jenger.riken.jp/en/result). In the BBJ, osteoporosis was defined on the basis of physicians' diagnoses in hospitals, and 7788 cases (696 men, 7092 women) aged 72.8 ± 10.1 years and 204 665 controls (108 651 men, 96 014 women) aged 61.6 ± 13.7 years were included in the study (35).

Gene Annotation and Enrichment Analysis

We annotated variants with ANNOVAR (36). Functional Mapping and Annotation (FUMA) was applied to identify candidate genes for each lead variant. Two gene-mapping criteria were compiled based on (1) physical distance (within a 10 000 base pair window from the known protein-coding genes) (37); and (2) significant expression quantitative trait locus (eQTL) association (GTEx v8 database, false discovery rate < 0.05) with the lead variant (38–40). Genomic Regions Enrichment of Annotations Tool (GREAT version 4.0.4) (41) and Metascape (https://metascape.org) (42) were applied to explore potential biological functional pathways. Significant (false discovery rate Q-value <0.05) enriched gene ontology (GO) biological terms and mouse phenotypes associated with significant signals were identified.

Statistical Analysis

Continuous variables were expressed as mean (SD) and Student's t tests were used to compare BMD means between men and women. Categorical variables were expressed as percentages. Phenotypic correlations between BMD at different sites were estimated using the Pearson correlation test. Correlations between BMD and covariates were estimated using the Pearson test for continuous variables and the Spearman correlation test for categorical variables. Cubic polynomial curves were generated for men and women separately to graphically represent BMD variation at each site with aging. Associations between the identified SNPs and height and weight were analyzed with linear models adjusting for age and sex. A 2-sided $P < .05$ was considered statistically significant. Analyses were conducted using R 3.4.4 software.

Power Analysis

We estimated the power to detect an effect of our study in total (n = 5428), and in men (n = 2364) and women (n = 3064). The power was estimated by dependence of the coefficient (beta) and the effect allele frequency usingQuanto software (version 1.2.4 from May 2009) (43). Parameters used for simulation were continuous (quantitative) phenotype, significance level

$\alpha = 5 \times 10^{-8}$, phenotype mean value 0.85, SD 0.15, additive genetic model, and no gene–environment interaction.

Results

Characteristics of the Study Population

The mean (SD) age of the 5428 participants was 63.5 (9.47) years (Table 1). There were 3064 (56.4%) women, among whom 2749 (89.7%) were postmenopausal. Men had higher mean BMD at all investigated sites than women (Table 1).

At about 45 years old, women did not have lower BMD at any site than men, but their BMD decreased dramatically afterwards, while men lost bone mass from about 65 years old (Fig. 2). In both sexes, BMD at the lumbar spine and intertrochanter was the highest, followed by total hip, femoral neck, and trochanter. BMD values at left sites and corresponding right sites were similar, with Pearson r values ranging between 0.72 and 0.94 (Fig. 2).

Heritability of BMD Varies by Site and Sex

The SNP heritability of BMD at different sites was about 0.27 to 0.39 in Model 1. Men had higher SNP heritability of BMD than women at the femoral neck (about 0.5 vs 0.4). The results did not show great change after further adjusting for height and weight in Model 2 (see Fig. S2 in (27)).

GWAS Reveals Novel Loci Associated With BMD

GWAS was performed for BMD at each of the 9 sites in the total population and when stratifying by sex (men and women). The Manhattan plots and QQ plots in Model 1 are presented elsewhere (Figs. S3-S8 in (27)). Conditional analysis found no new signals, and the results are presented elsewhere (Table S1 in (27)). A total of 6 loci were identified to be associated with BMD at any site (Fig. 3A), and 17q12-rs4795209 and 17q24.3-rs1239055408 were only significantly associated with BMD at the lumbar spine in men and at the right intertrochanter in women, respectively (see Table S1 (27)).

The Manhattan plots and QQ plots in Model 2 are presented elsewhere (Figs. S9-S14 in (27)). A total of 10 loci were identified to be associated with BMD at any site in Model 2 (Fig. 3B), and 7q11.21-rs79262027 was only significantly associated with BMD at the left femoral neck in men (see Table S1 in (27)).

The 2 models yielded 12 nonoverlapping loci that were associated with BMD at any site (Table 2). Regional association plots showed that most of the SNPs in high LD were also associated with BMD (see Fig. S15 (27)). The effects of the 12 loci on BMD of the significant site and stratum were comparable in Model 1 and Model 2, with ratios of beta values in Model 1 and Model 2 (a measure of the degree of attenuation of the BMD associations after further adjustment of height and weight) ranging between 0.85 and 1.38 (Fig. 4 and Table 2). Among the 12 loci, 1p36.12-rs72354346, 3p22.1-rs2024219, 4q22.1-rs1 463093, 5q14.3-rs10037512, 6q25.1-rs5880932, and 15q21 .2-rs730154 have been previously found to be associated with BMD mainly in Europeans, and the other 6 loci were novel (Table 2 and Table S2 in (27)). SNPs 3p22.1-rs2024219, 5q1 4.3-rs10037512, and 15q21.2-rs730154 were previously found to be associated with height (see Fig. S16 in (27)). SNP 5q1 4.3-rs10037512 was also associated with plateletcrit, fat-free mass, forced vital capacity, and balding type 1 (Table 2 and Table S2 in (27)). Notably, 7q11.21-rs79262027 G>A

Table 1. Basic characteristics of the study participants

	Overall (N = 5428)	Men (N = 2364)	Women (N = 3064)	P value
Age, years	63.5 (9.47)	64.5 (9.54)	62.7 (9.35)	<.001
Menopause, n (%)	—	—	2749 (89.7)	—
Height, cm	161.6 (8.30)	168.0 (6.34)	156.7 (5.91)	<.001
Weight, kg	63.49 (10.65)	69.13 (9.83)	59.13 (9.10)	<.001
BMI, kg/m^2	24.25 (3.30)	24.46 (3.10)	24.08 (3.44)	<.001
Bone mineral density, g/cm^2				
Lumbar spine	1.07 (0.19)	1.15 (0.18)	1.02 (0.17)	<.001
Total hip (L)	0.91 (0.14)	0.96 (0.13)	0.87 (0.14)	<.001
Total hip (R)	0.91 (0.15)	0.96 (0.15)	0.87 (0.14)	<.001
Femoral neck (L)	0.83 (0.14)	0.87 (0.13)	0.79 (0.14)	<.001
Femoral neck (R)	0.83 (0.15)	0.87 (0.15)	0.79 (0.13)	<.001
Trochanter (L)	0.73 (0.13)	0.80 (0.12)	0.68 (0.12)	<.001
Trochanter (R)	0.74 (0.13)	0.80 (0.12)	0.69 (0.12)	<.001
Intertrochanter (L)	1.09 (0.18)	1.14 (0.17)	1.05 (0.17)	<.001
Intertrochanter (R)	1.10 (0.18)	1.15 (0.18)	1.06 (0.17)	<.001

Data are presented as mean (SD) or n (%).

polymorphism only existed in EAS population, and 3q26.2-rs1 47371655 and 4q22.1-rs1463093 had higher minor allele frequencies in EAS than in other populations (Table 2).

Our power analysis showed that we had a power of 82.3% to detect a variant with effect allele frequency of 0.3 and an effect of 0.02 g/cm^2 in the total sample (see Fig. S17A in (27)). In sex-stratified analysis, the power to detect the effects of rs79262027 and rs4795209 in men and rs1239055408 in women was 12.4%, 89.3%, and 55.8% respectively (see Fig. S17B and C in (27)).

Three Variants Showed Sex-Heterogeneous Effects on BMD

For the identified significant SNPs, GWAMA software was used to test for sex-heterogenous effects. SNPs 17q12-rs4795209 and 7q11.21-rs79262027 had significantly stronger effects in men, and 17q24.3-rs1239055408 had significantly stronger effects in women (Fig. 4 and Table S3 in (27)).

In Silico Replication of the Lead SNPs in BBJ

We then looked up the lead SNPs in GWAS summary data of osteoporosis in the BBJ. SNPs 7q11.21-rs79262027, 9q21.12 -rs17522056, and 17q24.3-rs1239055408 or their proxy SNPs (LD r^2 > 0.6) were not found in BBJ, and 5 exact lead SNPs (1p36.12-rs72354346, 3p22.1-rs2024219, 4q22.1-rs1463093, 5q14.13-rs10037512, and 6q25.1 -rs5660932) were successfully replicated, with P values lower than .05 and the effect directions were the same as those in Changfeng (Table 3).

Next, we reviewed previous GWAS on BMD or osteoporosis in East Asian populations, and looked up their signals in the present study. Among the 16 lead SNPs identified in 6 studies, *JAG1*-rs2273061, *ESR1*-rs9371538, and *WNT16* -rs7776725 were significantly associated with BMD in the Changfeng population (see Table S4 in (27)); and *ESR1*-rs9371538 was in high LD (r^2 = 0.97) with our lead SNP rs5880932, implying the same signal.

Gene mapping and Pathway Enrichment Analysis

We identified 12 potential genes associated with BMD in which 5 genes had not been reported in previous BMD GWASs (see Table S5 in (27)). Five of the lead SNPs showed significant eQTL association with genes like *WNT4*, *SPP1*, and *CYP13A1* in hormone-related organs such as the thyroid and testis (Table S6 and Fig. 18 in (27)). Besides, we found that genes associated with the lead variants were highly enriched for the GO biological processes of ossification and regulation of secretion (Fig. 5A and Table S7 in (27)). Moreover, the lead variants were mainly enriched for abnormal bone resorption, increased osteoclast cell number, and kidney-related physiology among mouse phenotypes (Fig. 5B and Table S8 in (27)). These mapped genes were enriched in GWAS catalog reported gene sets, including BMD, lumbar spine BMD and, heel BMD (Fig. 5C and Table S9 in (27)).

Discussion

In the Shanghai Changfeng study with more than 5000 participants, we carried out GWASs of BMD measured using DXA at the lumbar spine, total hip, femoral neck, trochanter, and intertrochanter, and found that (1) 12 loci were significantly associated with BMD at any site, among which 1p36.12-rs7235 4346, 3p22.1-rs2024219, 4q22.1-rs1463093, 5q14.13-rs 10037512, and 6q25.1-rs5880932 were successfully replicated in osteoporosis GWASs in the BBJ, (2) the newly identified SNPs 7q11.21-rs79262027 and 17q12-rs4795209 were associated with BMD only in men, and 17q24.3-rs1239055 408 was associated with BMD only in women, (3) BMD in a Chinese elderly population was mainly related to ossification, bone resorption, hormone secretion, and kidney physiology.

Height and weight were included as covariates in some BMD GWASs (44) but not in others (11). However, adjusting for heritable covariates can bias effect estimates in GWASs, unless the tested variants have no effect on the covariate (45). Since height and weight were significantly associated with BMD in the Changfeng participants, we carried out 2
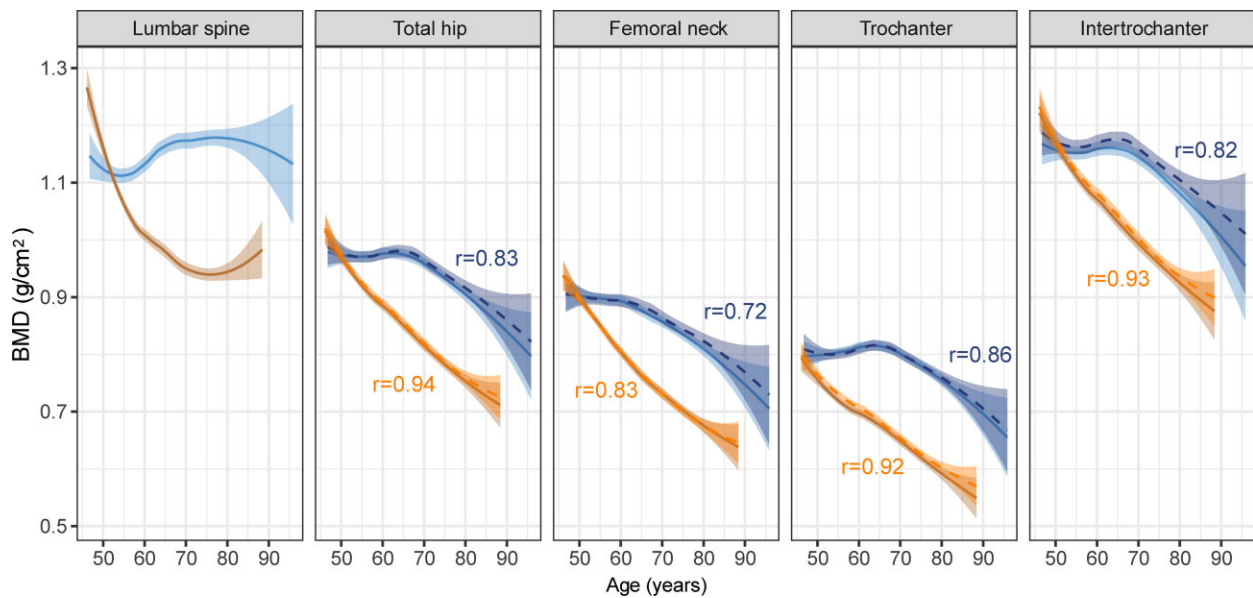
Figure 2. BMD variation at each site with aging in men and women. For the last 4 panels, solid lines represent the left site, and dashed lines represent right site.
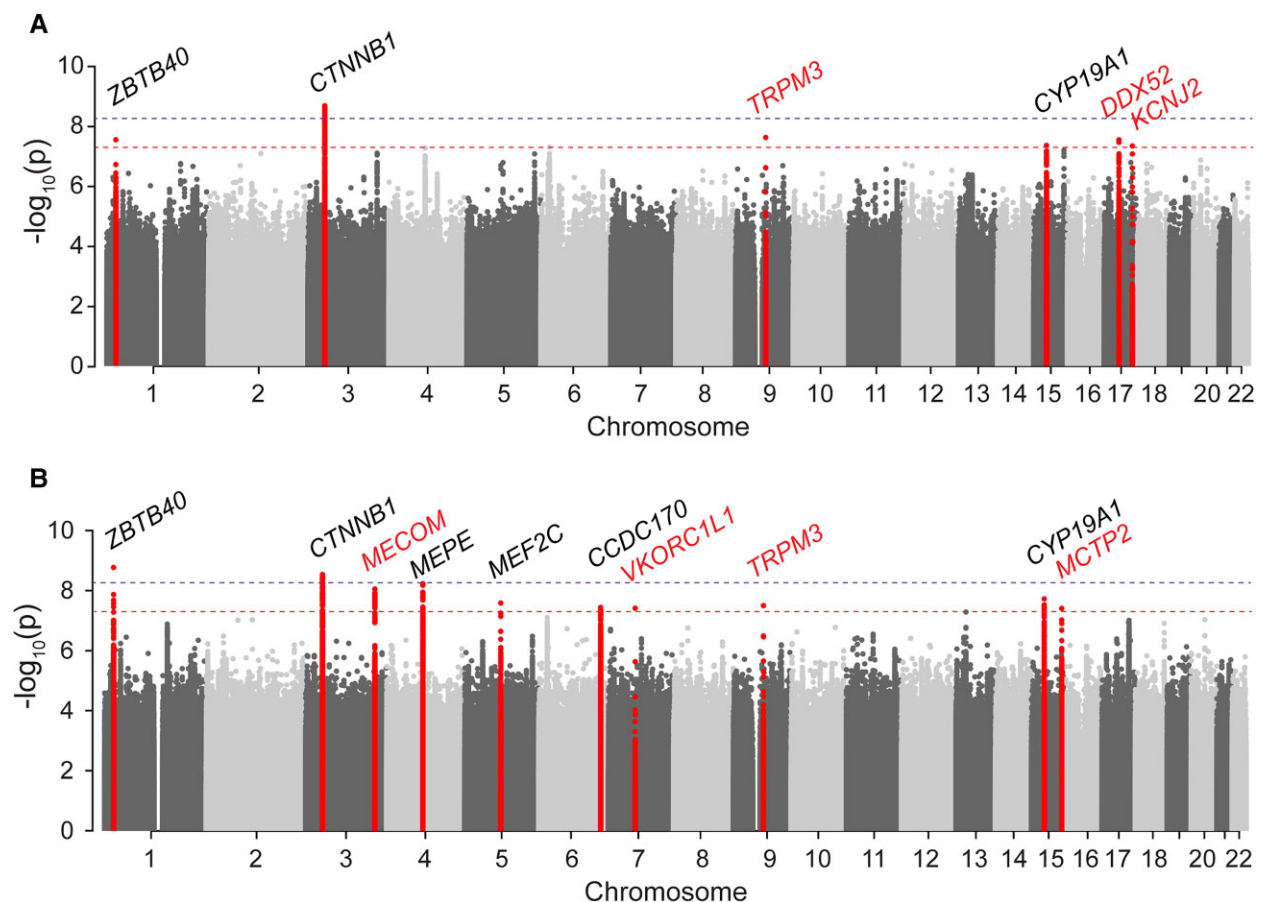

Figure 3. A Manhattan plot with combined results for association studies of BMD at different sites in combined and sex-stratified analyses in Model 1 (A) and Model 2 (B). Loci that have not previously found associated with BMD or osteoporosis are highlighted in red.

models (without and with adjustment of height and weight) in our BMD GWAS. As a result, although 3 of the identified 12 lead SNPs were previously reported to be associated with height, they were not significantly associated with height or weight of the Changfeng participants, and the estimated effects and P values were comparable in the 2 models. Therefore, we would not recommend that height and weight be adjusted in future BMD GWAS analysis. Otherwise, the

Table 2. Twelve nonoverlapping loci that were associated with BMD at any site in any stratum in the 2 models

Lead phenotype	Locus	SNP	POS	A1	A2	AF1	Associations with height			Associations with weight		
							Beta	SE	P	Beta	SE	P
(Total) femoral neck (R)	1p36.12	rs72354346[a]	22712923	G	GTCTCC	0.24	.000	0.001	.927	−.188	0.202	.351
(Total) trochanter (L)	3p22.1	rs2024219[b]	41146355	T	C	0.257	.000	0.001	.750	.168	0.198	.397
(Total) intertrochanter (L)	3q26.2	rs147371655	169293659	TA	T	0.344	−.001	0.001	.443	.091	0.182	.619
(Total) trochanter (L)	4q22.1	rs1463093[c]	88792520	T	C	0.282	.001	0.001	.291	.011	0.196	.956
(Total) femoral neck (R)	5q14.3	rs10037512[d]	88354675	T	C	0.404	.001	0.001	.174	.006	0.175	.970
(Total) trochanter (R)	6q25.1	rs5880932[e]	151892867	GA	G	0.493	.000	0.001	.655	.078	0.172	.653
(Men) femoral neck (L)	7q11.21	rs79262027	65269758	A	G	0.01	−.001	0.005	.849	−.626	0.844	.458
(Total) intertrochanter (L)	9q21.12	rs17522056	73737743	C	T	0.03	−.001	0.003	.680	.079	0.499	.874
(Total) lumbar spine	15q21.2	rs730154[f]	51591204	C	T	0.331	−.002	0.001	.139	.051	0.183	.782
(Total) trochanter (L)	15q26.1	rs11074227	94288155	T	A	0.338	.001	0.001	.337	−.077	0.183	.675
(Men) lumbar spine	17q12	rs4795209	35971028	G	A	0.139	−.001	0.001	.440	.250	0.243	.303
(Women) intertrochanter (R)	17q24.3	rs1239055408	68649015	GA	G	0.027	.003	0.003	.373	.828	0.519	.111

Nearest gene	Func_anno	AFR_AF	AMR_AF	EAS_AF	EUR_AF	SAS_AF
ZBTB40	Intergenic	0.228	0.108	0.25	0.118	0.159
CTNNB1	Intergenic	0.111	0.398	0.235	0.528	0.297
MECOM	Intronic	0.011	0.053	0.329	0.059	0.126
MEPE	Intergenic	0.134	0.098	0.271	0.066	0.045
MEF2C	Intronic	0.137	0.437	0.399	0.522	0.586
CCDC170	Intronic	0.154	0.285	0.499	0.131	0.262
VKORC1L1	Intergenic	0	0	0.009	0	0
TRPM3	Intronic	0.011	0.027	0.036	0.059	0.09
CYP19A1	Intronic	0.708	0.215	0.329	0.162	0.333
MCTP2	Intronic	0.299	0.415	0.355	0.522	0.296
DDX52	3′ UTR	0.089	0.219	0.144	0.208	0.236
KCNJ2	Intergenic	—	—	—	—	—

Model 1			Model 2 (height and weight adjusted)		
Beta	SE	P	Beta	SE	P
.015	0.003	2.92×10^{-8}	.015	0.002	1.69×10^{-9}
.015	0.003	2.15×10^{-9}	.014	0.002	3.56×10^{-9}
−.018	0.003	8.13×10^{-8}	−.018	0.003	8.81×10^{-9}
.013	0.002	5.47×10^{-8}	.013	0.002	5.86×10^{-9}
.012	0.002	1.68×10^{-7}	.012	0.002	2.58×10^{-8}
−.011	0.002	5.45×10^{-7}	−.011	0.002	3.61×10^{-8}
.080	0.018	6.36×10^{-6}	.094	0.017	3.84×10^{-8}
.051	0.009	2.46×10^{-8}	.048	0.009	3.14×10^{-8}
.019	0.003	4.50×10^{-8}	.019	0.003	1.88×10^{-8}
−.013	0.002	6.47×10^{-8}	−.012	0.002	3.91×10^{-8}
.042	0.008	2.95×10^{-8}	.036	0.007	5.12×10^{-7}
.066	0.012	4.70×10^{-8}	.048	0.011	1.71×10^{-5}

Abbreviations: BMD, bone mineral density; SNP, single nucleotide polymorphism; AF, allele frequency; AFR, African; AMR, American; EAS, East Asian; EUR, European; SAS, South Asian.

Previously found to be associated with:

[a]Heel BMD.

[b]BMD, osteoporosis, bone disorder, sitting height, standing height, spherical power, age started wearing glasses or contact lenses.

[c]BMD, uric acid.

[d]BMD, standing height, sitting height, forced vital capacity, forced expiratory volume in 1 second, plateletcrit, fat-free mass, alkaline phosphatase, balding type 1.
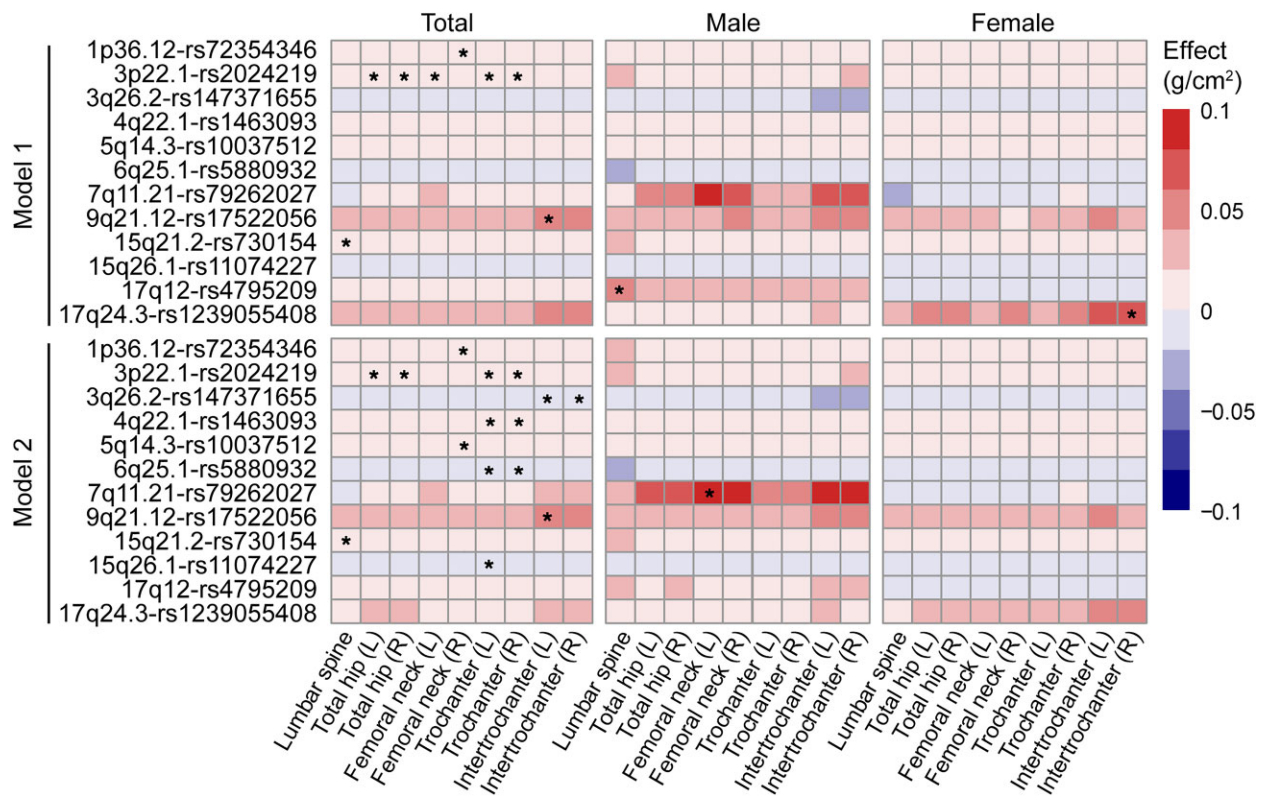
[e]Heel BMD, phosphate.

[f]Heel BMD, ALP, height.

Figure 4. Effect estimates of the associated lead SNPs on BMD at different sites in total population, men, and women. Asterisk represents $P < 5 \times 10^{-8}$.

Table 3. Effects of the identified lead SNPs in osteoporosis GWAS in BBJ project

Chr	SNP	Locus	POS	A1	A2	AF1	Beta	SE	P value
1	rs72354346	1p36.12	22712923	G	GTCTCC	0.268	−.055	0.02	**6.07 × 10⁻³**
3	rs2024219	3p22.1	41146355	T	C	0.221	−.042	0.022	**4.97 × 10⁻²**
3	rs147371655	3q26.2	169293659	TA	T	0.31	.02	0.019	2.93 × 10⁻¹
4	rs1463093	4q22.1	88792520	T	C	0.231	−.089	0.021	**1.44 × 10⁻⁵**
5	rs10037512	5q14.3	88354675	T	C	0.333	−.061	0.018	**8.55 × 10⁻⁴**
6	rs5880932	6q25.1	151892867	GA	G	0.498	.039	0.017	**2.45 × 10⁻²**
7	rs79262027	7q11.21	65269758	A	G	—	—	—	—
9	rs17522056	9q21.12	73737743	C	T	—	—	—	—
15	rs730154	15q21.2	51591204	C	T	0.411	−.008	0.018	6.35 × 10⁻¹
15	rs11074227	15q26.1	94288155	T	A	0.386	.012	0.019	5.14 × 10⁻¹
17	rs4795209	17q12	35971028	G	A	0.116	.039	0.027	1.46 × 10⁻¹
17	rs1239055408	17q24.3	68649015	GA	G	—	—	—	—

P < .05 are marked bold.

associations between the identified variants and the heritable covariates should be analyzed post-GWAS, and the results should be interpreted with caution.

SNPs rs72354346, rs2024219, rs1463093, rs10037512, rs5880932, and rs730154 were reported to be associated with BMD of participants in the UK Biobank and/or GEFOS (9–11, 46). In the present study, we found that they also have a significant genome-wide association with BMD in Chinese participants, and are nominally associated with osteoporosis diagnosed on the basis of BMD in the Japanese population (except for rs730154). This suggests overlapping mechanisms of bone metabolism in different ethnic groups. Few BMD or osteoporosis GWASs have been carried out in the EAS population (see Table S4 in (27)). Kung et al reported that rs2273061 mapping to *JAG1* was associated with BMD at the lumbar spine and femoral neck, and osteoporotic fracture in 800 unrelated southern Chinese women with extreme BMD (13), which was also nominally associated with lumbar spine BMD in the Changfeng participants. A GWAS of DXA-measured BMD in about 2700 Korean individuals
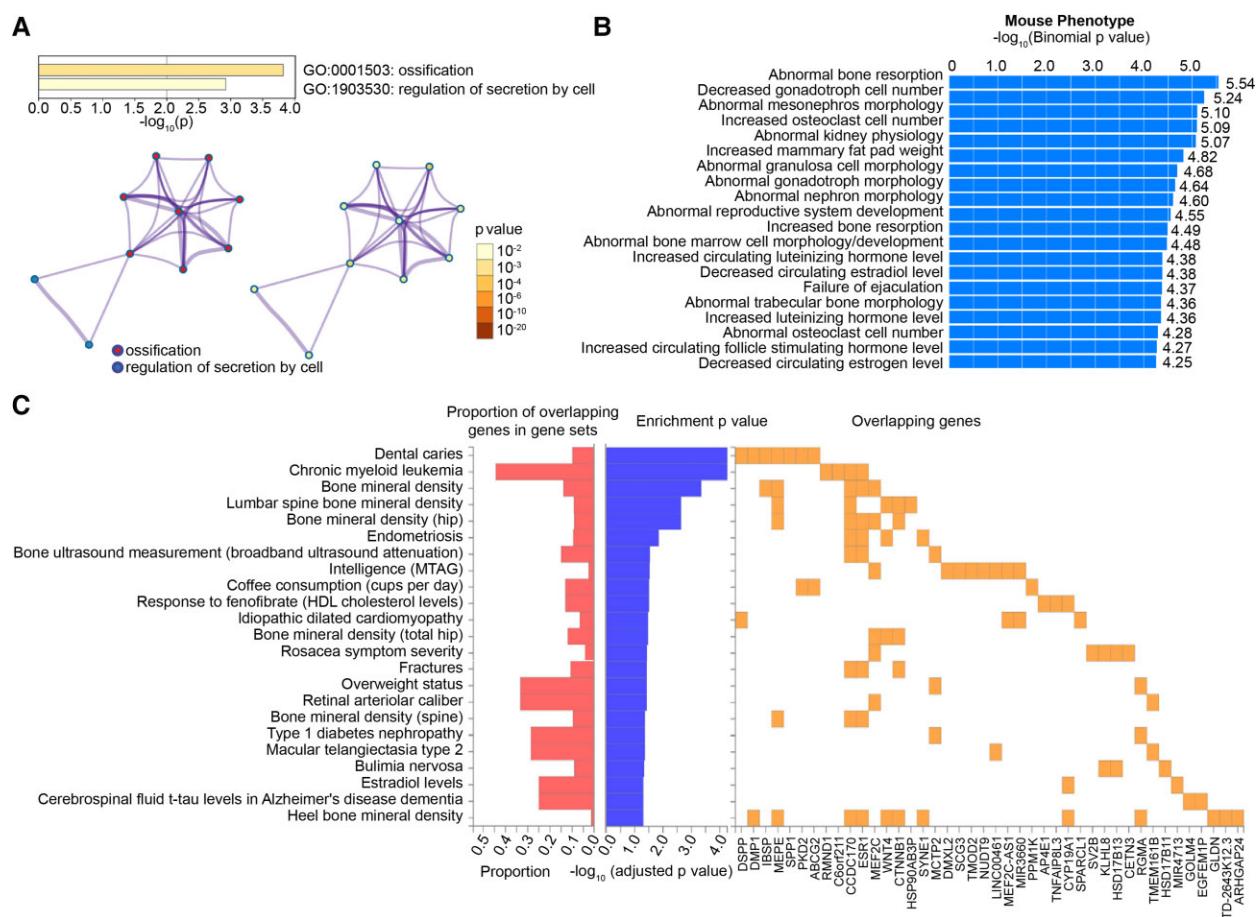
Figure 5. Enrichment analysis of lead variants. (A) Network of enriched GO Biological Processes by Metascape. Pathway enrichment analysis has been carried out with GO Biological Processes. All genes in the genome have been used as the enrichment background. Terms with a $P < .01$, a minimum count of 3, and an enrichment factor >1.5 (the enrichment factor is the ratio between the observed counts and the counts expected by chance) are collected and grouped into clusters based on their membership similarities. The lower left network is colored by cluster ID, where nodes that share the same cluster ID are typically close to each other. The lower right network is colored by P value, where terms containing more genes tend to have a more significant P value. (B) Mouse phenotype enrichment by GREAT. The test set of 12 genomic regions picked 20 (0%) of all 18 549 genes. The mouse phenotype has 9554 terms covering 9592 (52%) of all 18 549 genes, and 709 451 term–gene associations. (C) Enrichment of GWAS catalog reported genes by FUMA. See details elsewhere (Table S9 in (27)).

identified 4 signals (17), among which *ESR1*-rs9371538 was the same signal as *CCDC170*-rs5880932, and *WNT16*-rs7776725 was nominally significant in our study. Another 3 GWASs had been performed in an EAS population on osteoporotic fracture or osteoporosis (12, 14, 15), but none of the 3 reported SNPs was significant in our study. This might be due to the small sample sizes, or the fact that osteoporotic fracture is caused by not only low BMD but also many other factors such as sarcopenia, falls, and so on. Recently, a GWAS in 8842 Koreans reported 7 SNPs associated with osteoporosis diagnosed on the basis of distal radius BMD, with $P < 1 \times 10^{-5}$ but $> 5 \times 10^{-8}$ (46). Notably, rs9396260 and rs9464419 mapping to *ZNF451*, and rs10977574 and rs4390000 mapping to *PTPRD* were also associated with femoral neck BMD in our study. Together, future endeavors should be made on GWAS and replication on BMD in EAS populations with larger sample sizes.

Another 6 novel loci were identified in the present study. An interesting finding is that rs79262027 G>A near *VKORC1L1* was associated with BMD in men but not in women, and the polymorphism almost only existed in the EAS population. *VKORC1L1* (Vitamin K Epoxide Reductase Complex

Subunit 1 Like 1) encodes vitamin K oxidoreductase, which catalyzes the de-epoxidation of vitamin K 2,3-epoxide. The product vitamin K is important in the γ-carboxylation of glutamate residues of osteocalcin, which allows its binding to calcium and hydroxyapatite, and promotes bone formation (47). The function of *VKORC1L1* is currently not well reported (48). However, its paralog gene *VKORC1* was reported to play a role in BMD and osteoporosis (49, 50), and *VKORC1* SNPs were associated with BMD in non-Hispanic Black men and Mexican American men but not in women or non-Hispanic White people from NHANES III (51), which showed similar sex-specific effects on BMD to our findings on *VKORC1L1*. Therefore, *VKORC1L1* might be a susceptible gene of BMD specific to Asian men. Another novel signal is rs147371655 mapping to *MECOM*, which has a higher MAF (0.329) in EAS than in other populations. *MECOM* (MDS1 And EVI1 Complex Locus) encodes a transcription coactivator that regulates the differentiation and proliferation of hematopoietic stem cells, and *MECOM* mutations in humans may exhibit bone marrow failure, radioulnar synostosis, and other skeletal anomalies (52). Deletion of *Mecom* in mouse results in early-onset spinal deformity and osteopenia

(53). A GWAS meta-analysis in Koreans and Japanese people identified *MECOM* as a predisposing factor of osteoporotic fractures, and knockdown of *MECOM* by RNA interference suppresses osteoclastogenesis (15). However, the LD r^2 between rs147371655 in the present study and their lead SNP rs784288 is less than 0.001, which implies independent signals. SNP rs17522056 is a significant eQTL for *TRPM3* in brain in GTEX ($P = 6.4 \times 10^{-7}$). *TRPM3* (Transient Receptor Potential Cation Channel Subfamily M Member 3) is important for cellular calcium signaling and homeostasis. A functional experiment reported that agonists of *TRPM3* increased intracellular Ca^{2+} concentration from the extracellular space and RANKL protein expression in mouse osteoblastic cells (54). Unfortunately, they were not successfully replicated in the BBJ study. There might be several reasons: population heterogeneity in different environments and backgrounds, inconsistence of phenotype definitions (ie, BMD and osteoporosis), insufficient power (there is no significant variant in the GWAS of osteoporosis in the BBJ), or false positives.

The present study is to our knowledge the largest GWAS of BMD in an East Asian population. Limitations, however, exist. Firstly, the small sample size and insufficient power could have resulted in some true associations being unidentified. Secondly, we acknowledge the differences between the present GWAS and that of osteoporosis in the BBJ. We could find another replication cohort, but we hope these findings will provide possible clues for other researchers. Thirdly, the underlying mechanisms need further investigation after the novel loci have been validated.

In summary, this GWAS identified 12 loci associated with DXA-measured BMD in a middle-aged and elderly Chinese population, and 3 of them showed sex differences in their effects. These variations are related to ossification, bone resorption, hormone secretion, and kidney physiology.

Acknowledgments

Funding

Disclosure

The authors have nothing to disclose.

Data Availability

GWAS summary statistics are available from the corresponding authors upon reasonable request.

References

1. Genant HK, Cooper C, Poor G, *et al.* Interim report and recommendations of the World Health Organization task-force for osteoporosis. *Osteoporos Int.* 1999;10(4):259-264.
2. Wang Y, Tao Y, Hyman ME, Li J, Chen Y. Osteoporosis in China. *Osteoporos Int.* 2009;20(10):1651-1662.
3. Zeng Q, Li N, Wang Q, *et al.* The prevalence of osteoporosis in China, a nationwide, multicenter DXA survey. *J Bone Miner Res.* 2019;34(10):1789-1797.
4. Wu L, Lin H, Hu Y, *et al.* The major causes and risk factors of total and cause-specific mortality during 5.4-year follow-up: the Shanghai Changfeng study. *Eur J Epidemiol.* 2019;34(10):939-949.
5. Zhu X, Bai W, Zheng H. Twelve years of GWAS discoveries for osteoporosis and related traits: advances, challenges and applications. *Bone Res.* 2021;9(1):23.
6. Richards JB, Kavvoura FK, Rivadeneira F, *et al.* Collaborative meta-analysis: associations of 150 candidate genes with osteoporosis and osteoporotic fracture. *Ann Intern Med.* 2009;151(8):528-537.
7. Rivadeneira F, Styrkarsdottir U, Estrada K, *et al.* Twenty bone-mineral-density loci identified by large-scale meta-analysis of genome-wide association studies. *Nat Genet.* 2009;41(11):1199-1206.
8. Estrada K, Styrkarsdottir U, Evangelou E, *et al.* Genome-wide meta-analysis identifies 56 bone mineral density loci and reveals 14 loci associated with risk of fracture. *Nat Genet.* 2012;44(5):491-501.
9. Medina-Gomez C, Kemp JP, Trajanoska K, *et al.* Life-course genome-wide association study meta-analysis of total body BMD and assessment of age-specific effects. *Am J Hum Genet.* 2018;102(1):88-102.
10. Kemp JP, Morris JA, Medina-Gomez C, *et al.* Identification of 153 new loci associated with heel bone mineral density and functional involvement of GPC6 in osteoporosis. *Nat Genet.* 2017;49(10):1468-1475.
11. Morris JA, Kemp JP, Youlten SE, *et al.* An atlas of genetic influences on osteoporosis in humans and mice. *Nat Genet.* 2019;51(2):258-266.
12. Guo Y, Tan LJ, Lei SF, *et al.* Genome-wide association study identifies ALDH7A1 as a novel susceptibility gene for osteoporosis. *PLoS Genet.* 2010;6(1):e1000806.
13. Kung AW, Xiao SM, Cherny S, *et al.* Association of JAG1 with bone mineral density and osteoporotic fractures: a genome-wide association study and follow-up replication studies. *Am J Hum Genet.* 2010;86(2):229-239.
14. Kou I, Takahashi A, Urano T, *et al.* Common variants in a novel gene, FONG on chromosome 2q33.1 confer risk of osteoporosis in Japanese. *PLoS One.* 2011;6(5):e19641.
15. Hwang JY, Lee SH, Go MJ, *et al.* Meta-analysis identifies a MECOM gene as a novel predisposing factor of osteoporotic fracture. *J Med Genet.* 2013;50(4):212-219.
16. Tan LJ, Wang ZE, Wu KH, *et al.* Bivariate genome-wide association study implicates ATP6V1G1 as a novel pleiotropic locus underlying osteoporosis and age at menarche. *J Clin Endocrinol Metab.* 2015;100(11):E1457-E1466.
17. Choi HJ, Park H, Zhang L, *et al.* Genome-wide association study in East Asians suggests UHMK1 as a novel bone mineral density susceptibility gene. *Bone.* 2016;91:113-121.
18. Nieves JW. Sex-differences in skeletal growth and aging. *Curr Osteoporos Rep.* 2017;15(2):70-75.
19. Shanbhogue VV, Brixen K, Hansen S. Age- and sex-related changes in bone microarchitecture and estimated strength: a three-year

prospective study using HRpQCT. *J Bone Miner Res*. 2016;31(8): 1541-1549.

20. Gao X, Hofman A, Hu Y, *et al.* The Shanghai Changfeng study: a community-based prospective cohort study of chronic diseases among middle-aged and elderly: objectives and design. *Eur J Epidemiol*. 2010;25(12):885-893.

21. Purcell S, Neale B, Todd-Brown K, *et al.* PLINK: a tool set for whole-genome association and population-based linkage analyses. *Am J Hum Genet*. 2007;81(3):559-575.

22. Delaneau O, Coulonges C, Zagury JF. Shape-IT: new rapid and accurate algorithm for haplotype inference. *BMC Bioinformatics*. 2008;9:540.

23. Howie BN, Donnelly P, Marchini J. A flexible and accurate genotype imputation method for the next generation of genome-wide association studies. *PLoS Genet*. 2009;5(6):e1000529.

24. Zaitlen N, Kraft P, Patterson N, *et al.* Using extended genealogy to estimate components of heritability for 23 quantitative and dichotomous traits. *PLoS Genet*. 2013;9(5):e1003520.

25. Jiang L, Zheng Z, Qi T, *et al.* A resource-efficient tool for mixed model association analysis of large-scale data. *Nat Genet*. 2019; 51(12):1749-1755.

26. Zeng H, Ge J, Xu W, *et al.* Type 2 diabetes is causally associated with reduced serum osteocalcin: A genome-wide association and Mendelian randomization study. *J Bone Miner Res*. 2021;36(9): 1694-1707.

27. Zeng H, Ge J, Xu W, *et al.* Supplementary data for: Twelve loci associated with bone density in middle-aged and elderly Chinese: the Shanghai Changfeng Study. Zenodo. Deposited September 26, 2022. https://doi.org/10.5281/zenodo.7113903

28. Li J, Ji L. Adjusting multiple testing in multilocus analyses using the eigenvalues of a correlation matrix. *Heredity (Edinb)*. 2005;95(3): 221-227.

29. Mägi R, Morris AP. GWAMA: software for genome-wide association meta-analysis. *BMC Bioinformatics*. 2010;11:288.

30. Magi R, Lindgren CM, Morris AP. Meta-analysis of sex-specific genome-wide association studies. *Genet Epidemiol*. 2010;34(8): 846-853.

31. Yang J, Ferreira T, Morris AP, *et al.* Conditional and joint multiple-SNP analysis of GWAS summary statistics identifies additional variants influencing complex traits. *Nat Genet*. 2012;44(4):369-375.s361-363.

32. Boughton AP, Welch RP, Flickinger M, *et al.* Locuszoom.js: interactive and embeddable visualization of genetic association study results. *Bioinformatics*. 2021;37(18):3017-3018.

33. Kamat MA, Blackshaw JA, Young R, *et al.* Phenoscanner V2: an expanded tool for searching human genotype-phenotype associations. *Bioinformatics*. 2019;35(22):4851-4853.

34. Staley JR, Blackshaw J, Kamat MA, *et al.* Phenoscanner: a database of human genotype-phenotype associations. *Bioinformatics*. 2016;32(20):3207-3209.

35. Ishigaki K, Akiyama M, Kanai M, *et al.* Large-scale genome-wide association study in a Japanese population identifies novel susceptibility loci across different diseases. *Nat Genet*. 2020;52(7): 669-679.

36. Wang K, Li M, Hakonarson H. ANNOVAR: functional annotation of genetic variants from high-throughput sequencing data. *Nucleic Acids Res*. 2010;38(16):e164.

37. Watanabe K, Taskesen E, van Bochoven A, Posthuma D. Functional mapping and annotation of genetic associations with FUMA. *Nat Commun*. 2017;8(1):1826.

38. GTEx Consortium. The genotype-tissue expression (GTEx) project. *Nat Genet*. 2013;45(6):580-585.

39. Carithers LJ, Moore HM. The genotype-tissue expression (GTEx) project. *Biopreserv Biobank*. 2015;13(5):307-308.

40. Keen JC, Moore HM. The genotype-tissue expression (GTEx) project: linking clinical data with molecular analysis to advance personalized medicine. *J Pers Med*. 2015;5(1):22-29.

41. McLean CY, Bristor D, Hiller M, *et al.* GREAT Improves functional interpretation of cis-regulatory regions. *Nat Biotechnol*. 2010;28(5):495-501.

42. Zhou Y, Zhou B, Pache L, *et al.* Metascape provides a biologist-oriented resource for the analysis of systems-level datasets. *Nat Commun*. 2019;10(1):1523.

43. Gauderman W, Morrison J. QUANTO 1.1: a computer program for power and sample size calculations for genetic-epidemiology studies. 2006. Accessed November 18, 2008. http://hydra.usc.edu/gxe

44. Trajanoska K, Morris JA, Oei L, *et al.* Assessment of the genetic and clinical determinants of fracture risk: genome wide association and mendelian randomisation study. *BMJ*. 2018;362:k3225.

45. Aschard H, Vilhjálmsson BJ, Joshi AD, Price AL, Kraft P. Adjusting for heritable covariates can bias effect estimates in genome-wide association studies. *Am J Hum Genet*. 2015;96(2):329-339.

46. Bae JH, Park D. Effect of dietary calcium on the gender-specific association between polymorphisms in the PTPRD locus and osteoporosis. *Clin Nutr*. 2022;41(3):680-686.

47. Tsugawa N, Shiraki M. Vitamin K nutrition and bone health. *Nutrients*. 2020;12(7):1909.

48. Lacombe J, Ferron M. VKORC1L1, an enzyme mediating the effect of vitamin K in liver and extrahepatic tissues. *Nutrients*. 2018;10(8):970.

49. Holzer G, Grasse AV, Zehetmayer S, Bencur P, Bieglmayer C, Mannhalter C. Vitamin K epoxide reductase (VKORC1) gene mutations in osteoporosis: a pilot study. *Transl Res*. 2010;156(1): 37-44.

50. He J, Xie H, Yan C, Sun Y, Xu Z, Zhang X. Genetic variation in VKORC1 and risk for osteoporosis. *Arch Med Res*. 2021;52(2): 211-216.

51. Crawford DC, Brown-Gentry K, Rieder MJ. VKORC1 common variation and bone mineral density in the third national health and nutrition examination survey. *PLoS One*. 2010;5(12):e15088.

52. Germeshausen M, Ancliff P, Estrada J, *et al.* MECOM-associated syndrome: a heterogeneous inherited bone marrow failure syndrome with amegakaryocytic thrombocytopenia. *Blood Adv*. 2018;2(6):586-596.

53. Juneja SC, Vonica A, Zeiss C, *et al.* Deletion of Mecom in mouse results in early-onset spinal deformity and osteopenia. *Bone*. 2014;60:148-161.

54. Son A, Kang N, Kang JY, Kim KW, Yang YM, Shin DM. TRPM3/TRPV4 regulates Ca2+-mediated RANKL/NFATc1 expression in osteoblasts. *J Mol Endocrinol*. 2018;61(4):207-218.